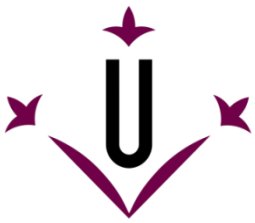

Protein/polysaccharide complexes to stabilize decane-in-water nanoemulsions

María Artiga-Artigas[2¤], Corina Reichert[1], Laura Salvia-Trujillo[2], Benjamin Zeeb[1], Olga Martín-Belloso[2], Jochen Weiss[1*]

*corresponding author

¤author to whom the correspondence should be addressed during the submission process

[1]Department of Food Physics and Meat Science, Institute of Food Science and Biotechnology, University of Hohenheim, Garbenstrasse 21/25, 70599 Stuttgart, Germany

[2]Department of Food Technology, University of Lleida – Agrotecnio Center, Av. Alcalde Rovira Roure 191, 25198. Lleida, Spain

Submitted to *<Food Biophysics>* on *<Month, Year>*

ABSTRACT

Protein/polysaccharide complexes can be formed by electrostatic interactions and may be useful for enhancing the stability of nanoemulsions containing short-chain alkanes, which are highly prone to destabilization by Ostwald ripening. The study aimed to assess the capacity of biopolymer complexes composed of whey protein isolate (WPI) and sugar beet pectin (SBP) to form and stabilize interfacially structured nanoemulsions. Nanoemulsions were stored for 21 days at room temperature to assess their stability against Ostwald ripening over time. Complexes showed higher emulsifying capacity than biopolymers alone since particle size of complex-stabilized nanoemulsions remained stable ($d_{4;3}$~0.26μm) for at least 48 h after preparation, whereas WPI- or SBP-stabilized nanoemulsions were prone to destabilization during the first 24 h reaching values around 1μm. Moreover, while the final particle size observed for the latter during the 21 days of storage was around 8μm, complex-stabilized nanoemulsions exhibited particle sizes up to 2.34μm, which had a direct impact in delaying creaming. Moreover, complex-stabilized nanoemulsions exhibited negative ζ-potential with similar values to those stabilized by SBP (-20.4 and -22.1mV, respectively) while the interfacial rheology behavior of complex-stabilized systems was more similar to those stabilized by WPI. This evidences that the protein fraction may be adsorbed at the oil interface thus dominating the interface rheology, whereas pectin chains located on the periphery of the complex and oriented towards the water phase may confer negative interfacial charge to oil droplets. These results indicated that WPI/SBP complexes were more effective than the biopolymers alone in preventing Ostwald ripening in decane-in-water nanoemulsions.

Keywords:

Whey protein; sugar beet pectin; protein/polysaccharide complexes; interfacial rheology

1. Introduction

Nanoemulsions have been described as colloidal dispersions of two immiscible phases (*e.g.* oil-in-water) with particle sizes up to 500 nm, which may act as carriers of lipophilic functional compounds including flavor oils or bioactive compounds [1]. In order to stabilize a dispersion of the oil droplets within the aqueous phase, molecules with surfactant capacity are needed to firstly reduce the interfacial tension between these two immiscible phases favoring nanoemulsions formation and subsequently allow their stabilization. Nonetheless, the major drawback of emulsion-based systems is their thermodynamic instability, so the presence of surfactants does not always guarantee the appearance of coalescence, flocculation or Ostwald ripening [2]. The most effective surfactants to avoid these destabilization phenomena are synthetic small-molecule weight surfactants [3]. However, scientists and manufacturers of food emulsions are nowadays focused on the replacement of synthetic emulsifiers by natural surface-active substances. In fact, there is a great interest in the food industry for using proteins (*e.g.* whey proteins, casein, gelatin, β-lactoglobulin, and insulin) and polysaccharides (*e.g.* gum arabic, intact or modified starches, pectins and alginates) to stabilize oil-in-water nanoemulsions [4–6].

On the one hand, proteins are known for their emulsification and foaming properties [7]. Specifically, dairy proteins such as whey protein isolates (WPI) have shown surfactant nature, electrostatic function and hydrophobic effect being able to adsorb at droplets interface avoiding oil droplets aggregation [8]. It is reported that the main proteins in WPI, which are β-lactoglobulin, α-lactalbumin and bovine serum albumin are

responsible for its interfacial properties [7]. On the other hand, polysaccharides, which have been originally incorporated during nanoemulsions formation for their water-holding and thickening properties, have also recently presented surfactant capacity. [9]. Pectins are anionic polysaccharides whose structure consists mainly of linear chains of galacturonic acid-containing acetyl groups within, phenolic esters in the side chains and proteinaceous moieties. Emulsion-stabilizing properties of pectins are well reported and attributed to the previously mentioned functional groups since they can act as additional anchors to the oil droplets enhancing pectin interfacial activity [10–12]. In this regard, sugar beet pectin (SBP), which is a type of pectin that exhibits a higher degree of acetylation and a greater branched structure compared to other conventional pectins, emerges as a potential alternative to be used as a natural surfactant [13]. Additionally, SBP also has a greater number of ferulic groups attached to the galactose and arabinose side chains and a greater amount of proteinaceous material bound to the lateral chains through covalent linkages [13]. Despite the existing evidence of the emulsion stabilizing properties of WPI and SBP, previously published studies have indicated that partially water-soluble lipids *e.g.* essential oils or short-chain alkanes *e.g.* decane are prone to suffer Ostwald ripening in the presence of natural biopolymers as single surfactant systems [2,14]. This is due to the low polarity of certain oils, thus tending to leak through the gaps that the surfactant leaves in the interface favoring that bigger droplets grow at the expense of those smaller provoking the breakdown of nanoemulsions [15]. Nonetheless, it has been reported that Ostwald ripening could be prevented or reduced when emulsifiers are sequentially or simultaneously used forming a thick and resistant interface. As such, several studies have recently demonstrated the surface-active capacity

of biopolymer complexes [16–18]. In general, the complexation of biopolymers is induced by electrostatic attraction forces between opposite charges [19–21]. The formation of protein/polysaccharide complexes has been well studied in terms of intrinsic and extrinsic parameters; however, their utilization as novel emulsifier systems to structure oil-in-water emulsions against Ostwald ripening is a relatively unexplored field.

Therefore, the purpose of this study was to investigate the impact of protein/pectin complexes (2% *w/w*) on the formation and stabilization of nanoemulsions containing 20% *w/w* decane as a model of low polarity oil. We hypothesized that interfacially adsorbed biopolymer complexes may form a thick and resistant interface and therefore prevent or retard oil droplets growth. Industrially relevant biopolymers, being WPI and SBP, were initially mixed under acidic conditions to allow complexation and subsequently emulsified using a high-pressure homogenizer. For the sake of clarity, single biopolymers were used as control samples. First, the electrostatic complexes were characterized in terms of electrical charge and microscopic images. Second, the stability of nanoemulsions stabilized by single biopolymers or the complex was assessed by determining their particle size, ζ-potential and particle growth. Additionally, accelerated creaming tests were performed. Lastly, the interfacial rheology of single biopolymers or the complex was studied.

2. Materials and methods

2.1 Materials

WPI was obtained from Fonterra GmbH (Hamburg, Germany). WPI is composed of a mixture of β-lactoglobulin, α-lactalbumin, bovine serum albumin, and other proteins. The pI of β-lactoglobulin is 5.3, whereas the pI of α-lactalbumin is 4.1, and thus the WPI has a pI close to 5 [22]. SBP was donated by Herbstreith & Fox KG (Neuenbürg, Germany). As stated by the manufacturer, the degree of methyl esterification of the beet pectin was 55%. Decane (purity > 99.0%) was obtained from Sigma-Aldrich Co. (Steinheim, Germany). Citric acid monohydrate, analytical grade hydrochloric acid (HCl), and sodium hydroxide (NaOH) were obtained from Carl Roth GmbH & Co. KG (Karlsruhe, Germany). Sodium citrate dihydrate was purchased from SAFC (St. Louis, MO). All biopolymers were used without further purification, whereas deionized water was used for the preparation of all samples.

2.2 Biopolymer complexation and characterization

Biopolymer complexes were generated and analyzed based on a previously published protocol [23]. Briefly, stock WPI and SBP solutions ($c_{biopolymer}$ = 2 %) were initially prepared at pH 7 and stirred overnight to ensure their complete hydration. Biopolymer solutions were then mixed at a WPI/SBP ratio of 1/1, whereas the pH was gradually decreased from 7 to 3. Biopolymer samples at several pHs (7, 6, 5, 4, 3.5 and 3) were collected and characterized in terms of ζ-potential and microstructure to determine the pH at which complexation occurs. ζ-potential measurements (Malvern Instruments Ltd, Worcestershire, UK) and optical microscopy (Axio Scope optical microscope A1, Carl

Zeiss Microimaging GmbH, Göttingen, Germany) were utilized to characterize the physicochemical properties of the complexes.

2.3 Formation of oil-in-water nanoemulsions with differently structured interfaces

Oil-in-water nanoemulsions having differently structured interfaces: (i) protein- or pectin-stabilized nanoemulsion (simple nanoemulsion) and (ii) complex-stabilized nanoemulsion were prepared. For the formation of aqueous emulsifier solutions 2% *w/w* WPI or SBP powder was dispersed into 10 mM sodium citrate buffer (pH 3.5). Both solutions were stirred overnight to ensure complete hydration of the biopolymer at room temperature and then readjusted to a pH of 3.5 using 1 M HCl and/or 1 M NaOH with a pH-meter (InoLab Level 1, Gemini, Apeldoorn, NL).

Single biopolymer-stabilized nanoemulsions were prepared by homogenizing 20% *w/w* of decane with 2% *w/w* WPI or SBP solutions using a high shear blender (Standard Unit, IKA Werk GmbH, Germany) at 15,000 rpm for 2 min followed by three passes at 1,000 bar (100 MPa) through a high pressure homogenizer (LM10, Microfluidics™, Westwood, MA). Nanoemulsions were kept at low temperature using an ice bath.

For the formation of complex-stabilized emulsions two stock solutions, one containing 2 % *w/w* of whey protein isolate (WPI) and the other 2 % *w/w* of sugar beet pectin (SBP), were prepared in citrate buffer (3.5 pH). Both solutions were magnetically stirred overnight to ensure complete hydration of the biopolymers at room temperature and pH was readjusted to 3.5. Afterward, both solutions were mixed 1/1 (WPI/SBP) ratio and 20% *w/w* of decane was added. The resulting mixture was homogenized by high-pressure homogenization as described earlier.

2.4 Characterization of nanoemulsions

2.4.1 Droplet size

The particle size distribution of nanoemulsions was determined during 21 days at room temperature using a static light scattering instrument (Horiba LA-950, Retsch Technology GmbH, Haan, Germany) and subsequently the mean droplet diameters were calculated. Samples were diluted in citrate buffer (pH 3.5) using a dilution factor of 1:200 sample-to-solvent to prevent multiple scattering effects. The refractive index (RI) was directly measured from decane-in-water nanoemulsions through the automated RI computation of the static light scattering device, which provided a value of 1.48. The particle size measurements are reported as volume frequency distributions and the mean diameters in terms of the volume ($d_{4;3}$) and number-based (d_{10}) mean diameters.

2.4.2 Droplet growth rate

Droplet growth during the time was monitored being is directly related to Ostwald ripening phenomenon. Droplet growth was modeled by the Lifshitz-Slyozov-Wagner (LSW) theory based on the assumption that the diffusion of oil through water determines the overall droplet growth rate [24]. The Ostwald ripening rate (ω) was calculated using the following equation:

$$\omega = \left(\frac{dr_c^3}{dt}\right)^3 = \frac{8\gamma^i D_0 C(\infty) V_m^2}{9RT} \qquad \textbf{eq.(1)}$$

where ω is the Ostwald ripening rate, r_c is the critical radius of a droplet; γ is the interfacial tension of decane ($5.23 \cdot 10^{-2}$ N/m); D_0 is the bulk diffusion coefficient for the decane in the continuous phase ($5.9 \cdot 10^{-10}$ m^2/s); $C(\infty)$ is the water solubility of decane ($3.6 \cdot 10^{-4}$ mol/m^2); V_m is its molar volume in m^3/mol; R is the molar gas constant (8.314 J/molK) and T is the standard temperature (20ºC) [15].

2.4.3 Optical microscopy

Particle size and particle growth during the time were confirmed by microscopy images taken periodically until day 21 of room temperature storage with an Axio Scope optical microscope (A1, Carl Zeiss Microimaging GmbH, Göttingen, Germany) working in dark field. All the studied samples were diluted in citrate buffer using a dilution factor of 1:30 sample-to-solvent before the microscopy analysis.

2.4.4 ζ -potential measurements

The ζ-potential (mV) was measured by phase-analysis light scattering (PALS) with a Zetasizer Nano-ZS laser diffractometer (Malvern Instruments Ltd, Worcestershire, UK). Samples were loaded into an appropriate cuvette and the ζ-potential was determined by measuring the direction and velocity that the droplets moved in the electric field applied. The Smoluchowski equation was utilized to calculate the ζ-potential. In all the determinations, samples were prior diluted in citrate buffer (3.5 pH) using a dilution factor of 1:30 sample-to-solvent.

2.4.5 Accelerated creaming index test

An accelerated creaming test was performed by centrifuging 2.5 mL aliquots of nanoemulsions, diluted to 1% in citrate buffer, using a Heraeus Centrifuge (Biofuge 28RS, Osterode, Germany). Samples were centrifuged at 2500 rpm during 1, 5, 10, 15, 30 or 50 min. Pictures of the emulsions were taken periodically with a digital camera (Canon Powershot G10, Tokyo, Japan) and the creaming index induced by centrifugation was calculated with equation (2):

$$\text{Creaming index } (\%) = (h_{\text{creaming (t)}} - h_{\text{creaming (t0)}})/h_{t0} * 100 \qquad \textbf{eq.(2)}$$

2.4.6 *Interfacial rheology*

Rheological measurements were conducted using a rheometer MCR 502 (Anton Paar GmbH, Graz, Austria; Software: Rheoplus) and were performed with a bicone measuring geometry, where the edge of the disk is located in the interfacial region between the two immiscible liquids. The influence of the bulk and upper phase of the flow field in the bicone system is compensated in an analysis performed using the rheometer software after the measurement. An amplitude sweep was conducted with 100 measuring points in the strain range between 0.01 to 100 % (frequency f = 0.01 Hz; ϑ = 25 °C). At the beginning of each measurement, a relaxation time of 15 min was applied. Each sample was measured in duplicate, whereas the interfacial storage modulus G_i' and loss modulus G_i'' were utilized as a key parameters to determine the rheological properties of the mixtures containing WPI solution (2% *w/w*), SBP solution (2% *w/w*) or complex WPI/SBP (1/1) solution (2% *w/w*) at pH 3.5 and decane as the upper fluid.

2.4.7 *Droplets interfacial density*

Interfacial density was theoretically calculated to determine the concentration of emulsifying biopolymers (*i.e.* WPI and/or SBP) adsorbed. This may contribute to elucidate the adsorption mechanism of WPI and/or SBP at oil/water interfaces, which is in turn linked to the understanding of Ostwald ripening phenomenon. For this purpose, the density of decane oil and decane-in-water nanoemulsions was measured using a Portable Density Meter (DMA™ 35, Anton Paar, Virginia, Ashland, USA). Equations (3-8) used for the theoretical calculation of droplets' interfacial density are available in the supplementary material.

2.5 Statistics

All the experiments were performed in duplicate, and at least three replicate analyses were carried out for each parameter. SigmaPlot 11.0 Systat Software was used to perform the analysis of variance. Tukey test was chosen to determine significant differences among the different emulsions, at a 5% significance level.

3. Results and discussion

3.1 Formation of WPI/SBP complexes

The formation of WPI/SBP complexes was accomplished following the methodology proposed by Zeeb et al. (2018). First of all, the changes in ζ-potential of single WPI and SBP solutions at varying pH were evaluated in order to determine their optimal electrical charge for electrostatic complex formation (Fig 1a). Subsequently, the formation of WPI/SBP complexes was assessed determining their ζ-potential (Fig 1a), microstructure (Fig 1b) and visual appearance (Fig 1c). WPI was negatively charged at high pH values (pH 7) and became positively charged below its isoelectric point (WPI pI ≈ 5) (Fig 1a). Nonetheless, pectin molecules, as well as the complex, remained negatively charged going from values of -40 to -25 mV as reducing the pH from 7 to 3 due to carboxylic groups of pectin may remain deprotonated at a wide range of pH values (Fig 1a). Indeed, at pH 3.5 the ζ-potential of WPI and SBP were respectively +28 mV and -22 mV being this pH the most favorable for the formation of WPI/SBP complexes. In fact, microscopic images showed that soluble complexes formation began at pH 5 and these complexes grew as the pH decreased (acidic conditions) leading to turbid solutions probably due to the increase of complexation strength (coacervates formation) (Fig 1b and 1c, respectively) [25,26]. However, complexes became insoluble at pH 3 thus

causing associative phase separation (Fig 1c). Thus, based on the observed results, the selected pH for the formation of WPI/SBP was 3.5.

3.2 Nanoemulsion stabilization by WPI/SBP complexes

3.2.1 Nanoemulsion characteristics and stability over time

The effectiveness of WPI/SBP complexes on nanoemulsions stabilization compared to biopolymers alone was evaluated. Therefore, mean droplet diameter in terms of $d_{4;3}$ and d_{10} (Table 1), particle size distribution (Fig 2) and particle size growth (Fig 3) of 20 % *w/w* decane-in-water nanoemulsions stabilized by WPI, SBP or their complex in a ratio 1/1 were measured by static light scattering. Samples were stored at room temperature and analyzed for 21 days. Subsequently, the microstructure in terms of optical microscopy and macrostructure regarding their visual appearance (Fig 4) of nanoemulsions were determined immediately after being prepared (day 0) and after 10 and 21 days of storage.

Nanoemulsion characterization

WPI/SBP complexes showed better capacity as emulsifiers in nanoemulsion formation compared to the biopolymers alone. Complex-stabilized nanoemulsions showed smaller particle sizes with values around 0.26 ± 0.07 μm, whereas those WPI or SBP-stabilized nanoemulsions presented particle size values higher than 0.31 μm (Table 1). This is in agreement with microscopic images of fresh nanoemulsions (t=0), which confirmed that their droplet size was initially in the nanometric range for all the studied samples thus being below the detection limit of the optical microscope (Fig 4a-c). Moreover, after nanoemulsions preparation (day 0), the three types of nanoemulsions (WPI-, SBP- or WPI/SBP-stabilized) showed a uniformly distributed dispersion of oil

droplets in the aqueous phase, regardless whether they were stabilized by the biopolymers alone or by the complex (Fig 2a-c).

Regarding the nanoemulsion electrical charge, those WPI/SBP complex- or SBP-stabilized showed negative charge at pH 3.5, with values of -22.1 ± 0.5 or -20.4 ± 0.5 mV respectively. In contrast, nanoemulsions stabilized with WPI presented positive ζ-potential with values of 37.5 ± 0.26 mV at this pH (Table 1). These differences can be explained due to WPI is a globular protein whose ζ-potential is slightly negative at physiological pH, yet it is able to change its net charge to positive while decreasing the pH [27]. The negative charge of pectin molecules has been previously attributed to the ionization of carboxylic groups, which in turn may promote intra-molecular self-association [28]. With regards to the complex-stabilized nanoemulsions, the negative charge of droplets stabilized by protein-pectin complexes may indicate that protein moieties of the complex may be primarily adsorbed at the o/w interface while pectin moieties may be potentially located at the outer region of the o/w interface.

Nanoemulsion stability

Nanoemulsions stabilized with SBP experienced an increase in the particle size from 0.37 ± 0.09 to 0.82 ± 0.04 µm during the first 24 h and continued growing until the appearance of a main intensity peak of oil droplets around 10 µm after 21 days of storage (Fig 2b). Likewise, WPI-stabilized nanoemulsions also presented a particle size increase from 0.31 ± 0.03 µm to 0.53 ± 0.02 µm during the first 24 h and reached values of 7.81 ± 0.72 µm after 21 days of storage (Fig 2a). Moreover, both SBP- and WPI-stabilized nanoemulsions showed a time-dependent increase of decane diffusion, which is indicative of Ostwald ripening according to the linear adjustment observed in Fig 3. Nonetheless,

according to the observed particle growth, Ostwald ripening of nanoemulsions stabilized with WPI was significantly slower and less pronounced than those containing SBP (Fig 3). This can be explained due to WPI is a globular protein that provides a thicker layer around the droplets and greater surface coverage of the interfacial area than SBP, which might slow down de Ostwald ripening [6,17,29]. Additionally, in spite of the dispersed oil droplets remained undetectable by optical microscopy until 10 days of storage, WPI- and SBP-stabilized nanoemulsions presented prominent destabilization after 21 days of storage (Fig 4a-b). After this period of storage, nanoemulsions stabilized by WPI showed a loose or porous three-dimensional structure with hollow regions of depleted oil droplets (Fig 4a). This structure may be the result of natural aggregation among droplets due to forces of mutual attraction known as London-Van der Waals that may predominate when droplet surfaces are close enough [30–32]. Indeed, macroscopic observations of the WPI-stabilized nanoemulsions after 21 days evidenced an irreversible phase separation with a thick and dense layer on the top of the tubes (Fig 4a'). Likewise, in the case of SBP-stabilized nanoemulsions, there was a remarkable presence of highly aggregated oil droplets with lipid-depleted areas after 21 days of storage followed by phase separation (Fig 4b and 5b). As mentioned in the previous section, instability of nanoemulsions containing SBP could be attributed to the placement that biopolymer adopts in the interface, which might favor lipid material diffusion, especially when it is relatively water-soluble as the decane. [33]. This is in agreement with Verkempinck et al. (2018), which observed that pectin molecules adsorbed at the same droplets interface may suffer repulsion since they are negatively charged leading to the formation of interfacial "uncovered gaps" through which the lipid material diffuses. Moreover, the observed

increment in the particle size of WPI- and SBP-stabilized nanoemulsions promoted flocculation which in turn, led to the emergence of creaming (Fig 4a'-b'). Indeed, Dickinson (1989) and Chanamai and McClements (2001) also reported that flocculation is able to cause several effects that are detrimental to emulsion quality including the enhancement of creaming.

Unlike SBP- and WPI-stabilized nanoemulsions, complex-stabilized nanoemulsions presented higher stability during storage. Indeed, complex-stabilized nanoemulsions presented slower and lesser changes in their particle size distribution (Fig 2) and particle growth (Fig 3), respectively. In fact, the particle size of complex-stabilized nanoemulsions remained stable (≈0.29 ± 0.03 μm) at least 48 h from their preparation and showed better emulsifying properties than WPI and SBP alone (Fig 2c). In addition, they exhibited the lowest increase in mean droplet diameter during the study, increasing up to 2.34 ± 0.86 μm after 21 days of storage. Although the slopes of the Ostwald ripening rate distribution of the complex- or WPI-stabilized nanoemulsions were similar, complexes resulted more efficient in delaying the particle size growth since the small particle population was maintained during more time (Fig 2 and 3, respectively). Therefore, WPI/SBP complexes might lead to denser interfaces due to hydrophobic interactions, altering interfacial rheology due to high internal stability of the interface and retarding the ripening process [18,37]. Nevertheless, in spite of the high surface activity of WPI/SBP complexes, they could not completely avoid the ripening process probably because they mostly behave like a soft polymer (Fig 3) [6]. Soft polymers are viscoelastic materials since they exhibit both elastic and viscous responses [38]. According to Chen, Wen, Janmey, Crocker, & Yodh (2010), the internal structures of these polymers can lead

to deformations in the interface of droplets in response to mechanical stresses favoring Ostwald ripening. Additionally, these soft polymers, such as WPI at pH bellow 4, may present a porous and weak gel flexible structure and exhibit a constant *G'* giving a linear response as will be proximately discussed in the interfacial rheology section [39]. Regarding the microstructure of complex-stabilized nanoemulsions, aggregation phenomenon was observed in day 21 (Fig 4c) agreeing with phase separation observed in Fig 4c'. This may also be attributed to the delay in particle growth, which suggests that in complex-stabilized nanoemulsions repulsion forces are higher preventing particles from coming together retarding flocculation and the subsequent phase separation [32].

3.2.2 Creaming index

An accelerated creaming test of nanoemulsions was conducted during different centrifugation times (0, 5, 10, 15, 30 and 45 min) at 2500 rpm. Rapid creaming was observed in WPI-stabilized emulsions, which reached a plateau after 15 min of centrifugation with a creaming index of 11% (Fig 5). In the case of SBP-stabilized nanoemulsions, the increase in the creaming index caused by centrifugation was progressive until reaching a constant value of 6% after 30 min of centrifugation (Fig 5). At the pH of the nanoemulsions (pH = 3.5), galactosyluronic acid residues from SBP chains are protonated and they may acquire compact conformations in which the hydrophobic groups can go towards the oil interface and adsorb [28]. Therefore, the interface may consist of a mixture of different functional groups and the applying of external forces such as centrifugation may modify the conformational characteristic of biopolymers thus altering the stability [40]. In both cases, creaming could be attributed to flocculation phenomenon since centrifugation causes a partial phase separation due to a

biopolymer concentration gradient [41]. Centrifugation generates zones with low biopolymer concentrations, in which its adsorption is insufficient to yield full surface coverage [41,42]. Thus, once WPI or SBP were excluded from droplets interface due to centrifuge forces, they may favor flocculation and irreversible creaming formation.

In complex-stabilized nanoemulsions, the increase of the induced creaming index reached a plateau value (1.5%) after 10 minutes of centrifugation (Fig 5). Therefore, WPI/SBP complexes seem to be effective in preventing creaming even at room temperature. This can be related to the fact that in complex-stabilized nanoemulsions, charged functional groups from both biopolymers are interacting among them forming the complex, so there are fewer intermolecular interactions. In this regard, droplets may be closer to each other after centrifugation thus leading to a thinner cream layer since there are fewer spaces between them.

3.2.3 Interfacial rheology

Interfacial rheology measurements were performed to elucidate the adsorption mechanisms of the different emulsifiers used at decane droplet interfaces. Interfacial rheology studies the relationship between the deformation of a liquid interface and different forces as a function of time [43]. Interfacial characteristics depend on the behavior of the molecules located at the interface including their chemical composition, concentration and interactions [44]. The interfacial storage modulus (G_i') and the interfacial loss modulus (G_i") determine interfacial rigidity and both contributions constitute the interfacial shear modulus. G_i' represents the recoverable energy stored in the interface, whereas the loss modulus, G_i", accounts for energy lost both through shear dissipation processes [45].

On the one hand, the interfacial shear modulus (G_i' and G_i'') of WPI at the decane interface remained constant at increasing strain amplitude (Fig 6a). It is reported that proteins adsorb at fluid-fluid interfaces by forming a highly interconnected network at the surface of decane stabilized by hydrogen bonds, hydrophobic and electrostatic interactions and specific covalent bonds between molecules [46]. Nonetheless, this adsorption may depend on the polarity of the oil and also on concentration and type of the biopolymer and the interface aging time, defined as the static storage time wherein interface formation takes place [43]. Therefore, the lack of an interconnected network observed in our interfacial rheology results might suggest that the aging time was not enough for the entire formation of the WPI monolayer. Actually, in the study performed by Erni et al. [47], results were collected after 20 h of aging since longer intervals for recording and averaging have proven beneficial effects in terms of interfacial measurements performance.

Shear rheology measurements of SBP-decane interfaces showed higher values of G_i' compared to those of G_i'' as well as a decay in the G_i' and G_i'' with increasing amplitude after the latter reached a maximum. This behavior, which is characteristic of soft glassy materials and has been attributed to the balance between the breaking and formation of bonds, suggests that the resulting interfacial network generated is elastic (Fig 6b) [48]. In agreement with our results, Gromer et al. (2009) and Rodriguez Patino & Pilosof (2011) also observed that SBP was able to form elastic or viscoelastic films at the air/water or oil/water interface, respectively. The interfacial elasticity has been attributed to the high hydrophobicity of pectin [4]. Indeed, acetyl groups of SBP, which enhance its hydrophobic nature and surface-active character favor the formation of elastic interfaces

[37]. This interface is susceptible to deform at low pH due to a lack of electrostatic repulsive forces between pectin chains causing weak steric repulsion [49].

Interfacial rheology similarities between WPI- and complex-stabilized nanoemulsions (Fig 6a and c, respectively) reinforced the previously drawn hypothesis that protein moieties of the complex are adsorbed at the interface leaving the pectin moieties oriented towards the bulk aqueous phase. Indeed, it is reported that complexes may adsorb directly at oil interfaces due to the interaction of protein moieties from their outside with the decane and the pectin remained linked to these adsorbed protein molecules [37]. The obtained results concerning interfacial rheology suggested, on the one hand, that probably longer aging times are necessary to allow the complete adsorption of WPI at decane interface; and on the other hand, that changes in the protein/pectin ratio would modify the properties of the interface.

3.2.4 Theoretical calculation of interfacial density

A plausible explanation for the higher emulsification and emulsion stabilization capacity of WPI/SBP complexes in comparison to the biopolymers alone might be attributed to the fact that they form a denser layer at the oil/water interface. Therefore, the interfacial density of the different nanoemulsions was theoretically calculated with equations 3-8 (supplementary material). For this purpose, the three following assumptions were taken into account: (*i*) the shape of droplets is spherical; (*ii*) every droplet has the same diameter being monodisperse; and (*iii*) all biopolymer molecules are located at the interface. The interfacial densities of WPI-, SBP- and complex-stabilized nanoemulsions were not significantly different after the theoretical calculations with values of $0.026 \pm 2 \cdot 10^{-4}$, $0.026 \pm 8 \cdot 10^{-4}$ and $0.025 \pm 4 \cdot 10^{-3}$, respectively (Table 2). It may

be due to that the concentration of biopolymer molecules per unit of interfacial surface was the same in all nanoemulsions whether the emulsifier is a single biopolymer or a complex. In general, the mass of biopolymer that is adsorbed at the interface depends on several factors including interactions between the biopolymer and the oil, which in turn will determine the conformation of biopolymer when adsorbed. Siew et al. [33] reported that 1 mg/m^2 is enough for WPI to form a monolayer at the oil/water interface, whereas they determined that the required amount of adsorbed SBP onto limonene oil droplets was ~9.5 mg/m^2. In this regard, the higher stability of the complex-stabilized nanoemulsions in comparison with the biopolymers alone might be related to the compactness of the complex at the interface rather than the number of adsorbed molecules of the interfacial layer.

4. Conclusion

The WPI/SBP complexes presented an improved behavior as emulsifiers and stabilizers in nanoemulsions formulated with short alkanes in comparison with the single biopolymers, showing higher prevention of Ostwald ripening thus retarding droplet growth. In fact, complex-stabilized nanoemulsions remained stable during 48 h, whereas those single-stabilized nanoemulsions exhibited almost immediate destabilization after their preparation. Moreover, the adsorption mechanism of WPI/SBP complex could be elucidated according to the assessed physicochemical parameters. In this regard, the oil/water interface electrical charge of the complex-stabilized nanoemulsions was similar to that of the SBP-stabilized nanoemulsions; whereas its interfacial rheology was similar to that of the WPI-stabilized emulsions. This evidenced that the protein moieties of the complex adsorb at the oil droplet surface thus dominating the viscoelastic properties of

the interface whereas the pectin moieties are oriented towards the bulk aqueous phase thus governing the electrical characteristics of the oil droplets. This work contributes towards understanding the behavior of biopolymer-based emulsifiers such as protein/pectin complexes at oil/water interfaces and to elucidate their capability of stabilizing nanoemulsions containing short alkanes. Hence, these results might be of importance when designing interfacial strategies for the stabilization of nanoemulsions containing lipid phases with relatively high water solubility, such as short-chain fatty acids or essential oils as delivery systems of active compounds.

Acknowledgments

This study was funded by the Ministry of Economy, Industry and Competitiveness (MINECO/FEDER, UE) throughout project **AGL2015-65975-R**. Author María Artiga-Artigas thanks the University of Lleida for their pre-doctoral fellowship. Author Laura Salvia-Trujillo thanks the "Secretaria d'Universitats i Recerca del Departament d'Empresa i Coneixement de la Generalitat de Catalunya" for the Beatriu de Pinós post-doctoral grant **BdP2016 00336**.

The authors declare that they have no conflict of interest.

5. References

1. C. G. Otoni, R. J. Avena-Bustillos, C. W. Olsen, C. Bilbao-Sáinz, and T. H. McHugh, **57**, 72 (2016).

2. S. Suriyarak and J. Weiss, Colloids Surfaces A Physicochem. Eng. Asp. **446**, 71 (2014).

3. D. J. McClements, L. Bai, and C. Chung, Annu. Rev. Food Sci. Technol. **8**,

(2017).

4. O. E. Pérez, C. Carrera Sánchez, A. M. R. Pilosof, and J. M. Rodríguez Patino, J. Food Eng. **94**, 274 (2009).

5. M. Evans, I. Ratcliffe, and P. A. Williams, Curr. Opin. Colloid Interface Sci. **18**, 272 (2013).

6. E. Dickinson, Food Hydrocoll. **23**, 1473 (2009).

7. R. Baeza, C. Carrera Sanchez, A. M. R. Pilosof, and J. M. Rodríguez Patino, Food Hydrocoll. **19**, 239 (2005).

8. J. Yi, T. I. Lam, W. Yokoyama, L. W. Cheng, and F. Zhong, J. Agric. Food Chem. **62**, 8900 (2014).

9. M. Artiga-Artigas, M. I. Guerra-Rosas, J. Morales-Castro, L. Salvia-Trujillo, and O. Martín-Belloso, Food Hydrocoll. **81**, 209 (2018).

10. M. & L. 2002 Akhtar, Dickinson, Food Hydrocoll. **17**, 455 (2002).

11. T. Funami, G. Zhang, M. Hiroe, S. Noda, M. Nakauma, I. Asai, M. K. Cowman, S. Al-Assaf, and G. O. Phillips, Food Hydrocoll. **21**, 1319 (2007).

12. M. Nakauma, T. Funami, S. Noda, S. Ishihara, S. Al-Assaf, K. Nishinari, and G. O. Phillips, Food Hydrocoll. **22**, 1254 (2008).

13. M. Rejaii and E. A. Salehi, Int. J. PharmTech Res. **9**, 364 (2016).

14. A. Chebil, J. Desbrières, C. Nouvel, J. L. Six, and A. Durand, Colloids Surfaces A Physicochem. Eng. Asp. **425**, 24 (2013).

15. B. Zeeb, M. Gibis, L. Fischer, and J. Weiss, J. Colloid Interface Sci. **387**, 65 (2012).

16. A. Gromer, A. R. Kirby, A. P. Gunning, and V. J. Morris, Langmuir **25**, 8012

(2009).

17. A. K. Ghosh and P. Bandyopadhyay, The Complex World of Polysaccharides 395 (2012).

18. B. Zeeb, L. Mi-Yeon, M. Gibis, and J. Weiss, Food Hydrocoll. **74**, 53 (2018).

19. K. J. Klemmer, L. Waldner, A. Stone, N. H. Low, and M. T. Nickerson, Food Chem. **130**, 710 (2012).

20. S. Liu, C. Elmer, N. H. Low, and M. T. Nickerson, Food Res. Int. **43**, 489 (2010).

21. C. Schmitt and S. L. Turgeon, Adv. Colloid Interface Sci. **167**, 63 (2011).

22. E. Dickinson, J. Chem. Soc. Faraday Trans. **88**, 2973 (1992).

23. B. Zeeb, C. Stenger, J. Hinrichs, and J. Weiss, Food Struct. **10**, 10 (2016).

24. J. Santos, N. Calero, L. A. Trujillo-Cayado, M. C. Garcia, and J. Muñoz, Colloids Surfaces B Biointerfaces **159**, 405 (2017).

25. J. L. Doublier, C. Garnier, D. Renard, and C. Sanchez, Curr. Opin. Colloid Interface Sci. **5**, 202 (2000).

26. B. Chen, H. Li, Y. Ding, and H. Suo, LWT - Food Sci. Technol. **47**, 31 (2012).

27. E. Ruffin, T. Schmit, G. Lafitte, J. M. Dollat, and O. Chambin, Food Chem. **151**, 324 (2014).

28. K. Alba and V. Kontogiorgos, Food Hydrocoll. **68**, 211 (2017).

29. J. Combrinck, A. Otto, and J. du Plessis, AAPS PharmSciTech **15**, 588 (2014).

30. A. Teo, K. K. T. Goh, J. Wen, I. Oey, S. Ko, H. S. Kwak, and S. J. Lee, Food Chem. **197**, 297 (2016).

31. T. Harnsilawat, R. Pongsawatmanit, and D. J. McClements,

Biomacromolecules **7**, 2052 (2006).

32. D. L. Forbes, WET USA [on Line] (2014).

33. C. K. Siew and P. A. Williams, J. Agric. Food Chem. **56**, 4164 (2008).

34. S. H. E. Verkempinck, C. Kyomugasho, L. Salvia-trujillo, S. Denis, M. Bourgeois, A. M. Van Loey, M. E. Hendrickx, and T. Grauwet, Food Hydrocoll. **85**, 144 (2018).

35. E. Dickinson, Colloids and Surfaces **42**, 191 (1989).

36. R. Chanamai and D. J. McClements, J. Food Sci. **66**, 457 (2001).

37. J. M. Rodriguez Patino and A. M. R. Pilosof, Food Hydrocoll. **25**, 1925 (2011).

38. D. T. N. Chen, Q. Wen, P. A. Janmey, J. C. Crocker, and A. G. Yodh, Annu. Rev. Condens. Matter Phys. **1**, 301 (2010).

39. Q. Tang, (1993).

40. L. M. Chevalier, L. E. Rioux, P. Angers, and S. L. Turgeon, Food Hydrocoll. **87**, 61 (2019).

41. D. Guzey and D. J. McClements, Adv. Colloid Interface Sci. **128–130**, 227 (2006).

42. E. Dickinson, M. G. Semenova, A. S. Antipova, and E. G. Pelan, Food Hydrocoll. **12**, 425 (1998).

43. M. A. Bos and T. Van Vliet, Adv. Colloid Interface Sci. **91**, 437 (2001).

44. J. Pelipenko, J. Kristl, R. Rošic, S. Baumgartner, and P. Kocbek, Acta Pharm. **62**, 123 (2012).

45. E. M. Freer, K. S. Yim, G. G. Fuller, and C. J. Radke, J. Phys. Chem. B **108**, 3835 (2004).

46. B. S. Murray, Curr. Opin. Colloid Interface Sci. **7**, 426 (2002).

47. P. Erni, P. Fischer, E. J. Windhab, V. Kusnezov, H. Stettin, and J. Läuger, Rev. Sci. Instrum. **74**, 4916 (2003).

48. A. Torcello-gómez and T. J. Foster, Carbohydr. Polym. **113**, 53 (2014).

49. K. Alba, L. M. C. Sagis, and V. Kontogiorgos, Colloids Surfaces B Biointerfaces **145**, 301 (2016).

Figure 1

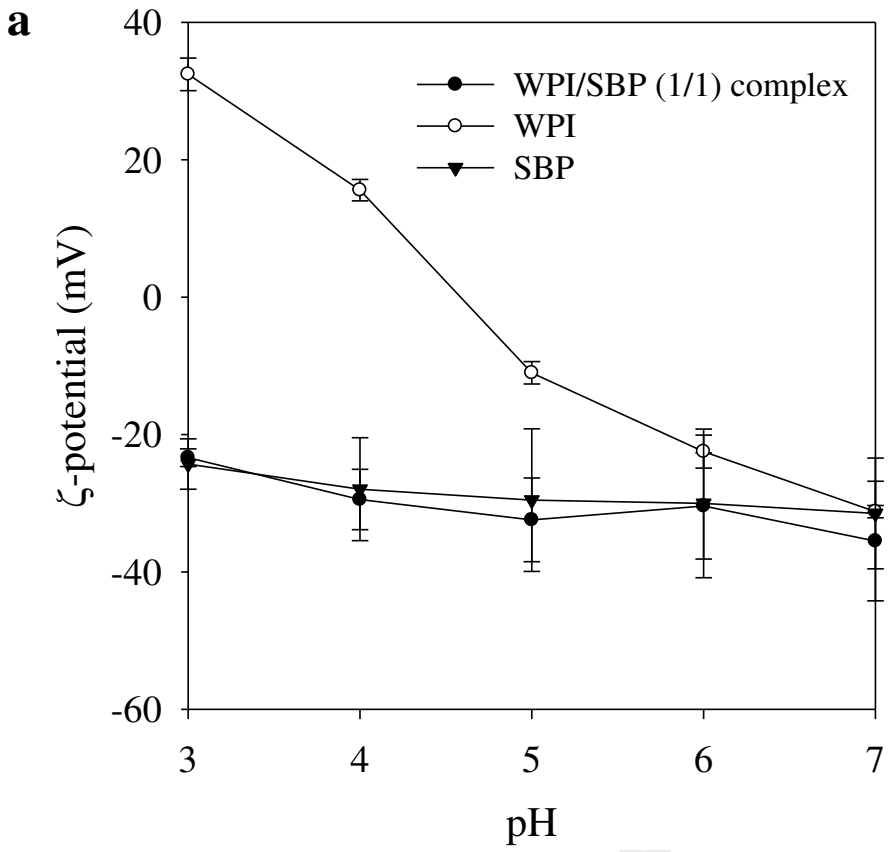

b

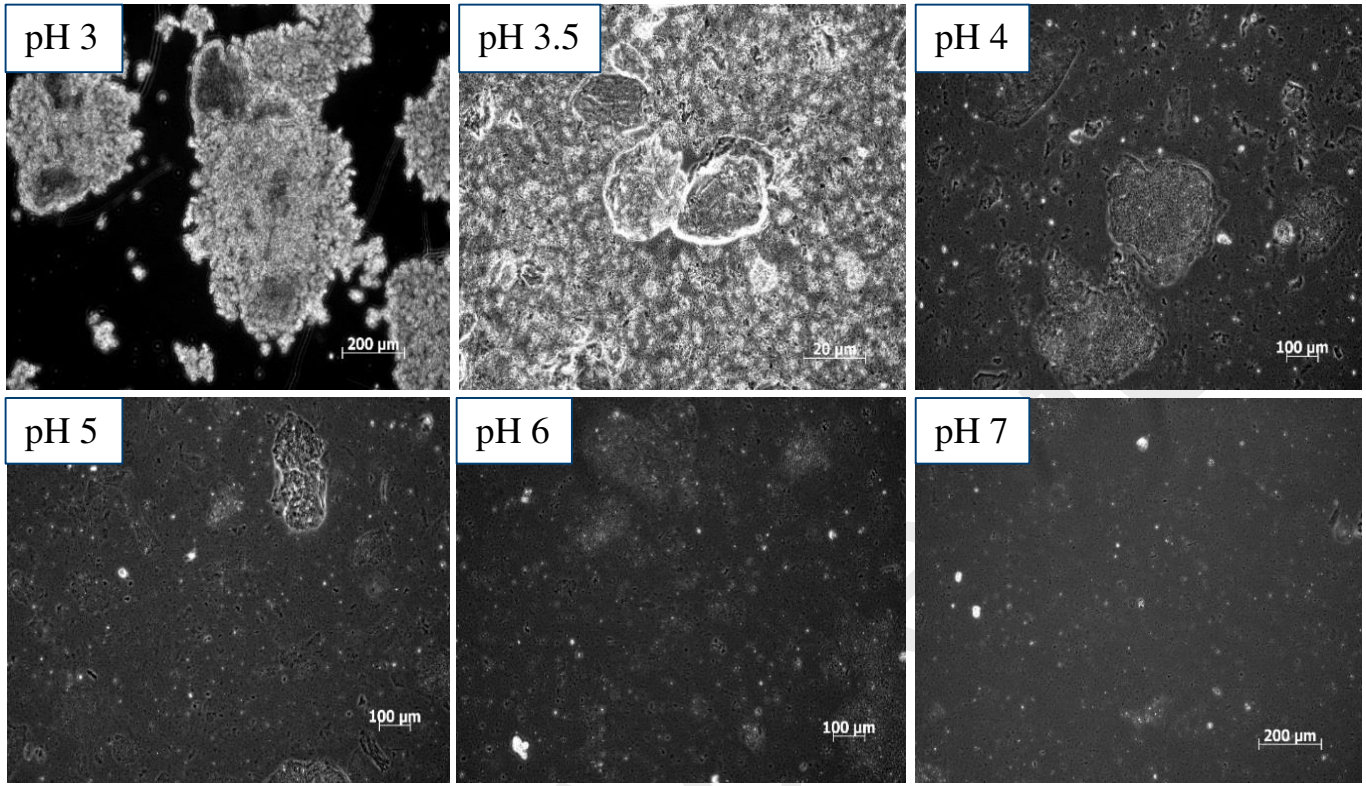

c

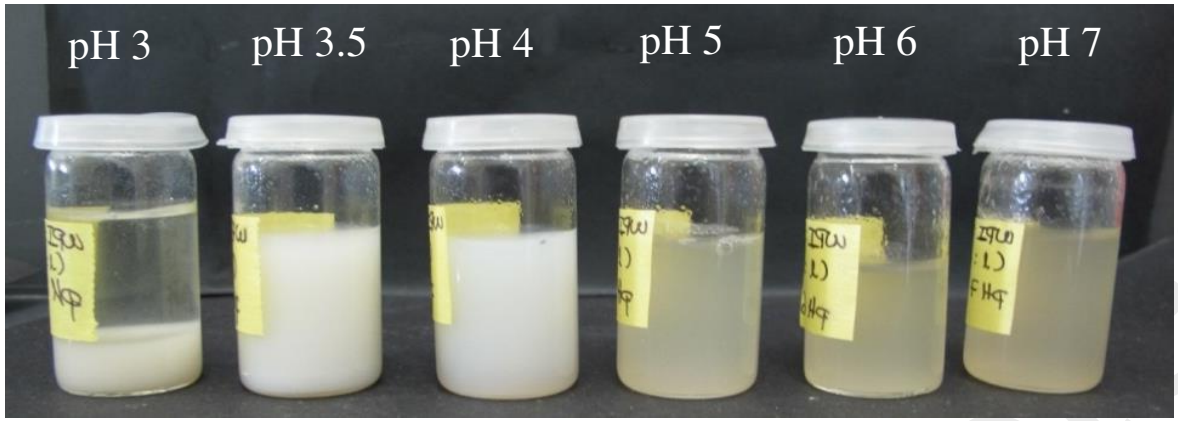

Fig 1 Change in the ζ-potential (mV) of whey protein isolate (WPI), sugar beet pectin (SBP) and WPI/SBP complex formation in distilled water by varying the pH from 7 to 3 **(a)**; optical microstructure of WPI/SBP (1/1) complexes from pH 3 to 7 **(b)**; outward appearance of complexes during their formation **(c)**.

Figure 2

a

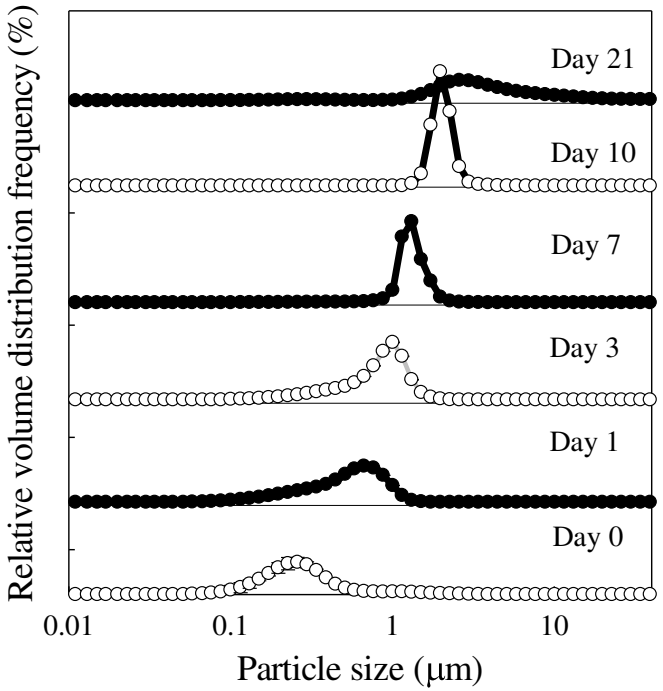

b

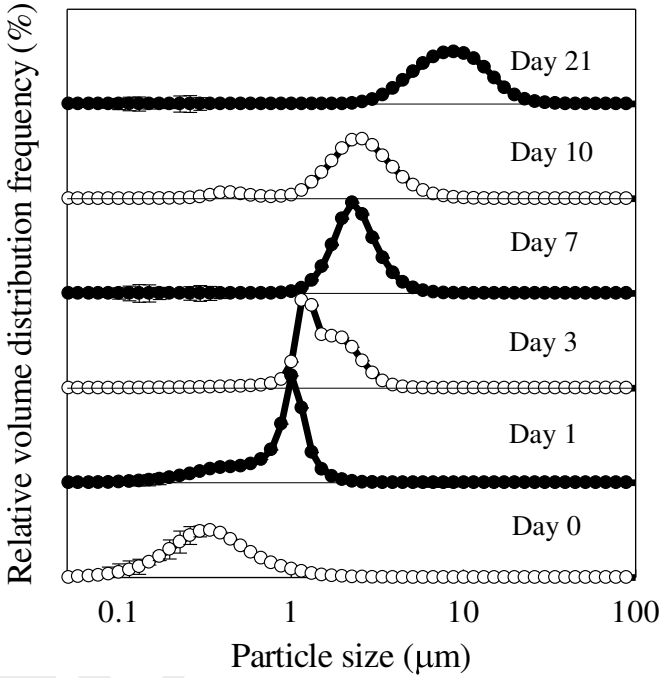
Relative volume distribution frequency (%)
Day 21
Day 10
Day 7
Day 3
Day 1
Day 0
0.1
1
10
100
Particle size (μm)

c

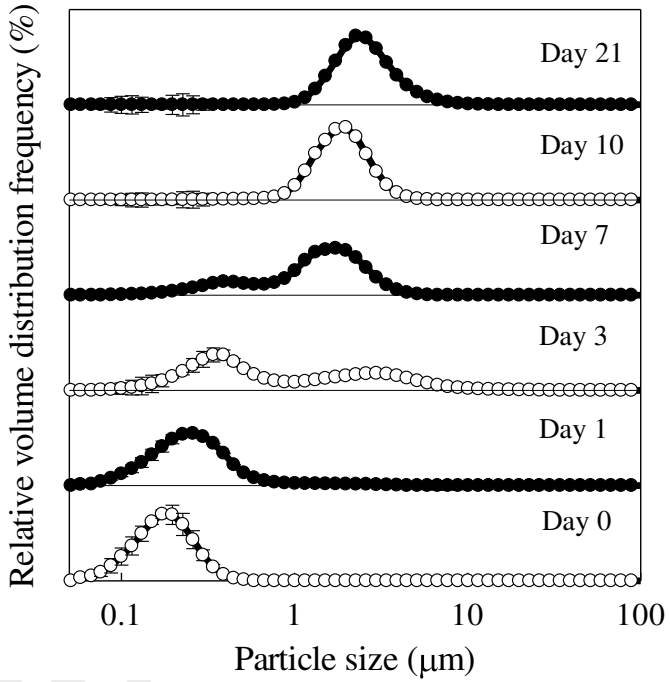

Fig 2 Particle size distribution of nanoemulsions containing 2% *w/w* Whey Protein Isolate (WPI) **(a)**, 2% *w/w* of Sugar Beet Pectin (SBP) **(b)** or 2% *w/w* of the WPI/SBP (1/1) complex **(c)**, acting as emulsifiers; and 20% *w/w* of decane as oil phase during 21 days.

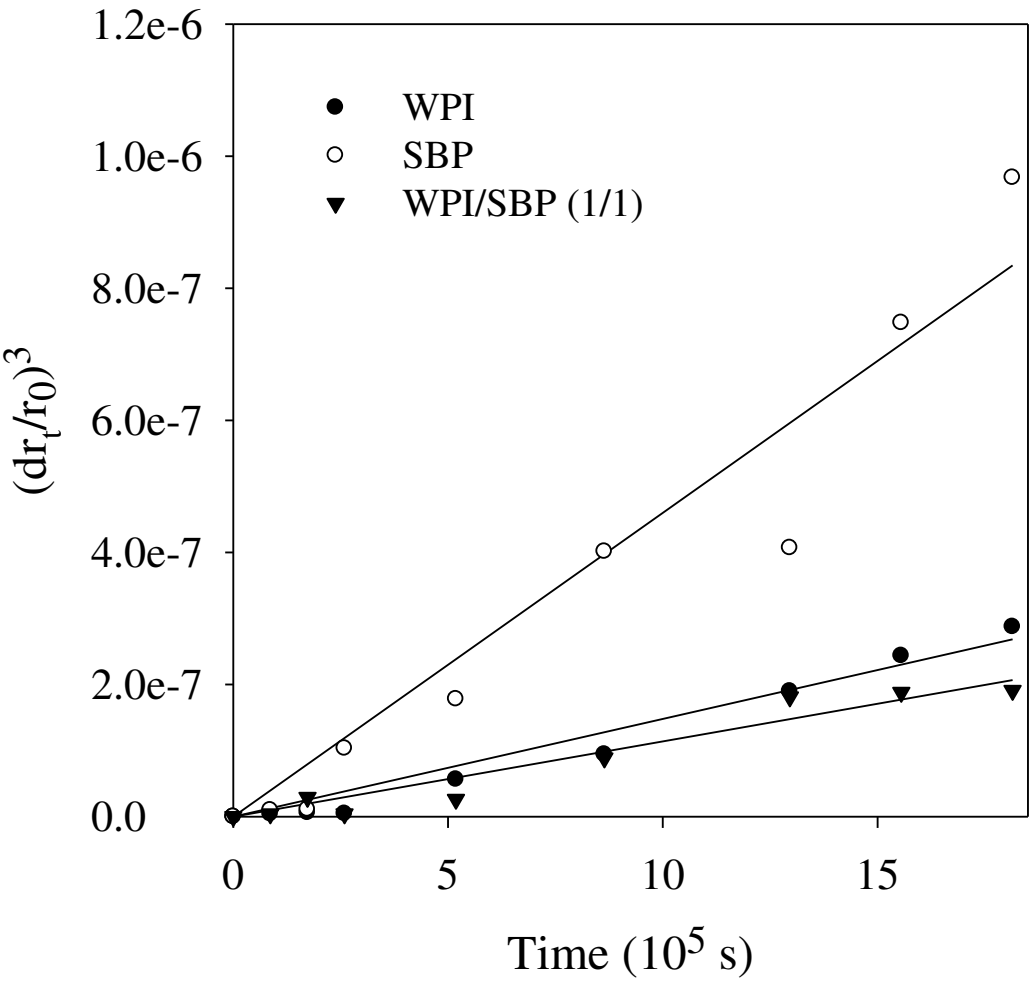

Fig 3 Impact of interfacial structure (biopolymer 2 % *w/w*) on the time-dependent growth of decane-in-water nanoemulsions (20 % *w/w* decane) stabilized by whey protein isolate (WPI), sugar beet pectin (SBP), and WPI/SBP complexes.

Figure 4

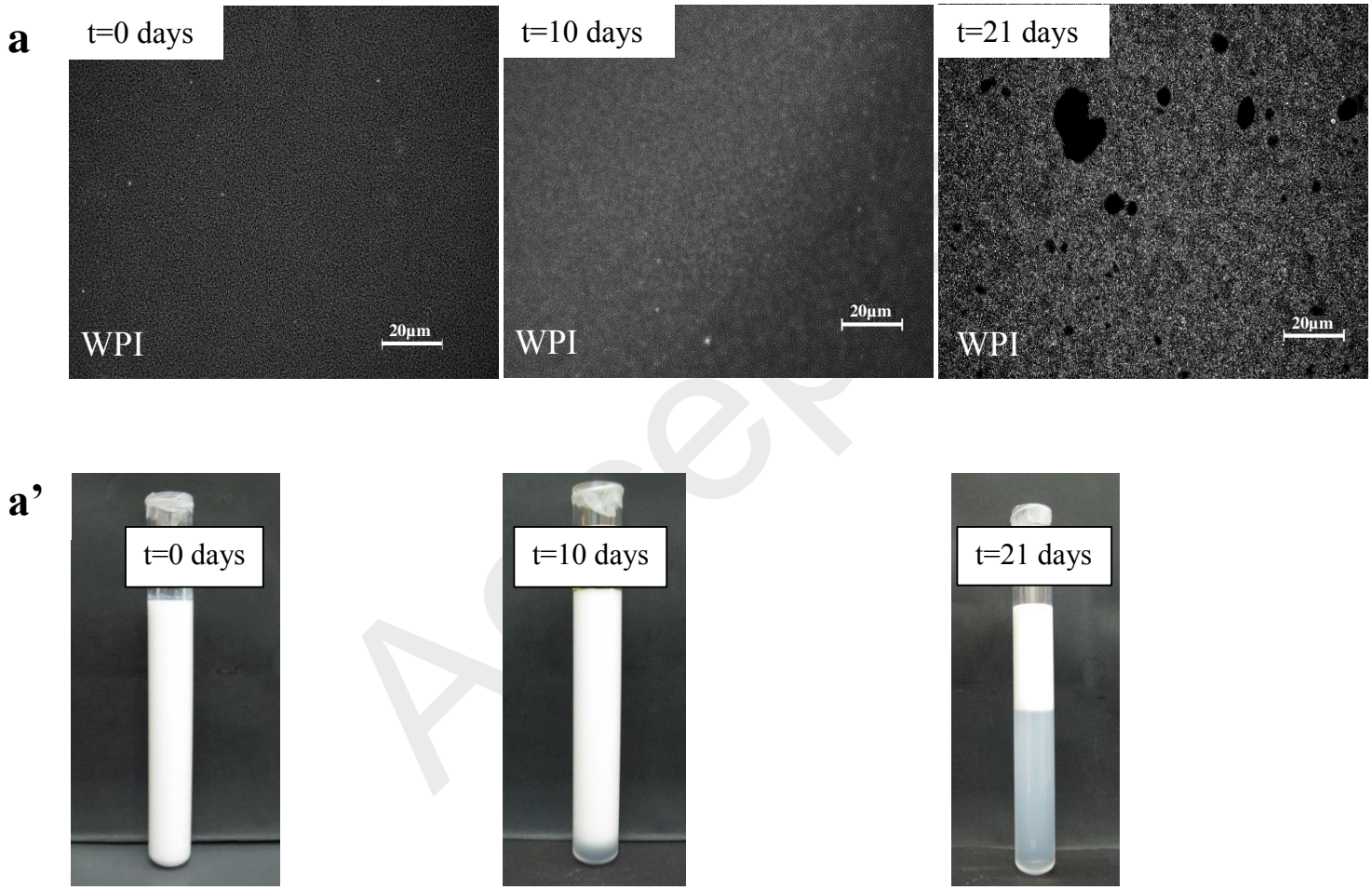

b

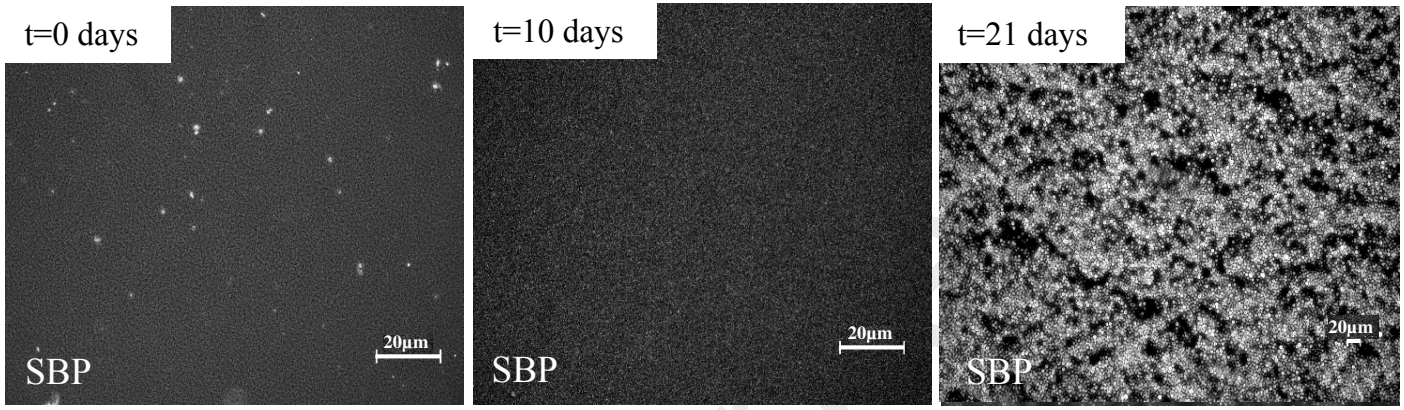
t=0 days
SBP
20µm
t=10 days
SBP
20µm
t=21 days
SBP
20µm

b'

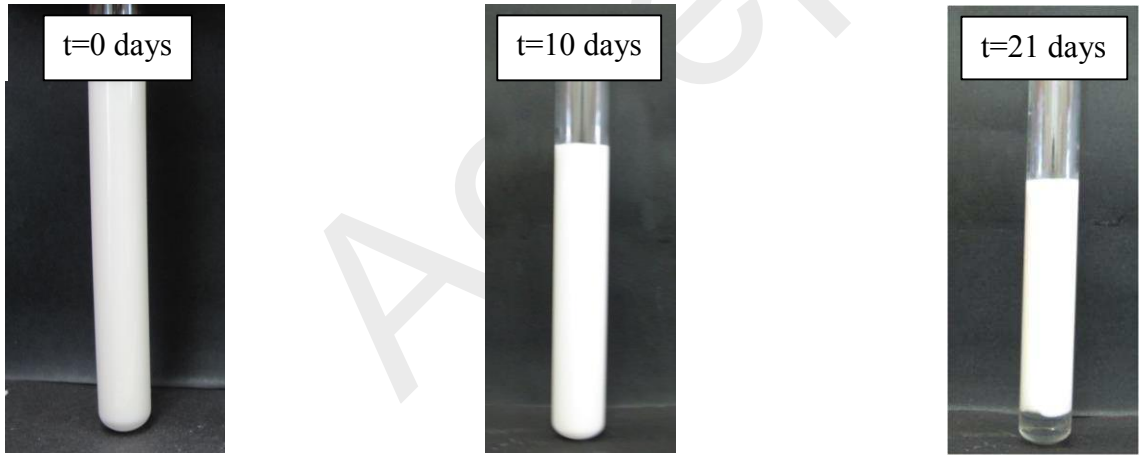
t=0 days
t=10 days
t=21 days

c

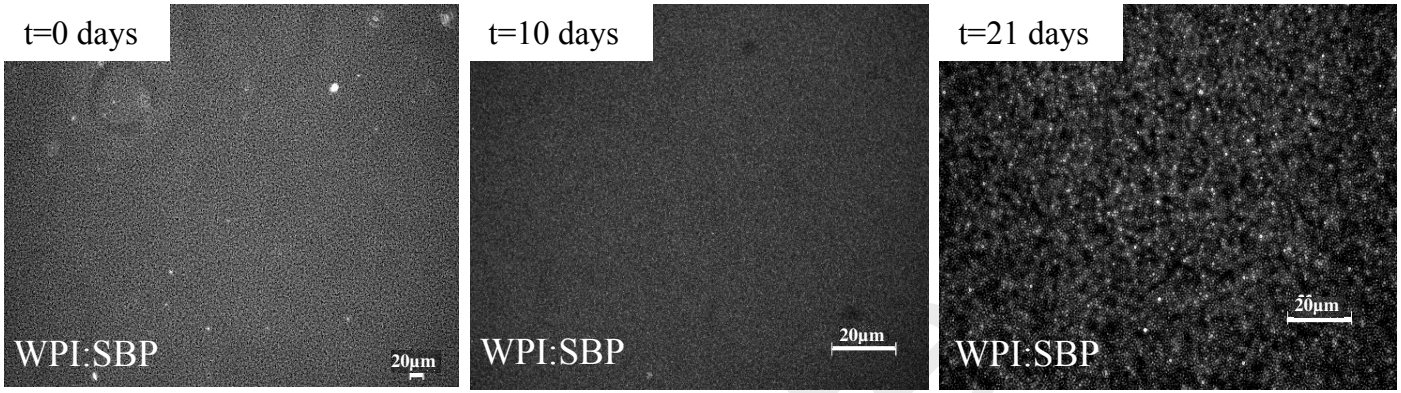
t=0 days
WPI:SBP
20µm
t=10 days
WPI:SBP
20µm
t=21 days
WPI:SBP
20µm

c'


t=0 days
t=10 days
t=21 days

Fig 4 Optical microstructure **(a, b or c)** and pictures **(a', b' or c')** of decane-in water nanoemulsions stabilized by whey protein isolate (WPI), sugar beet pectin (SBP) or WPI/SBP (1/1) complex, respectively, during 21 days of room temperature storage. Samples for microscopic measurements were diluted in citrate buffer in a ratio 1:30 sample-to-solvent.

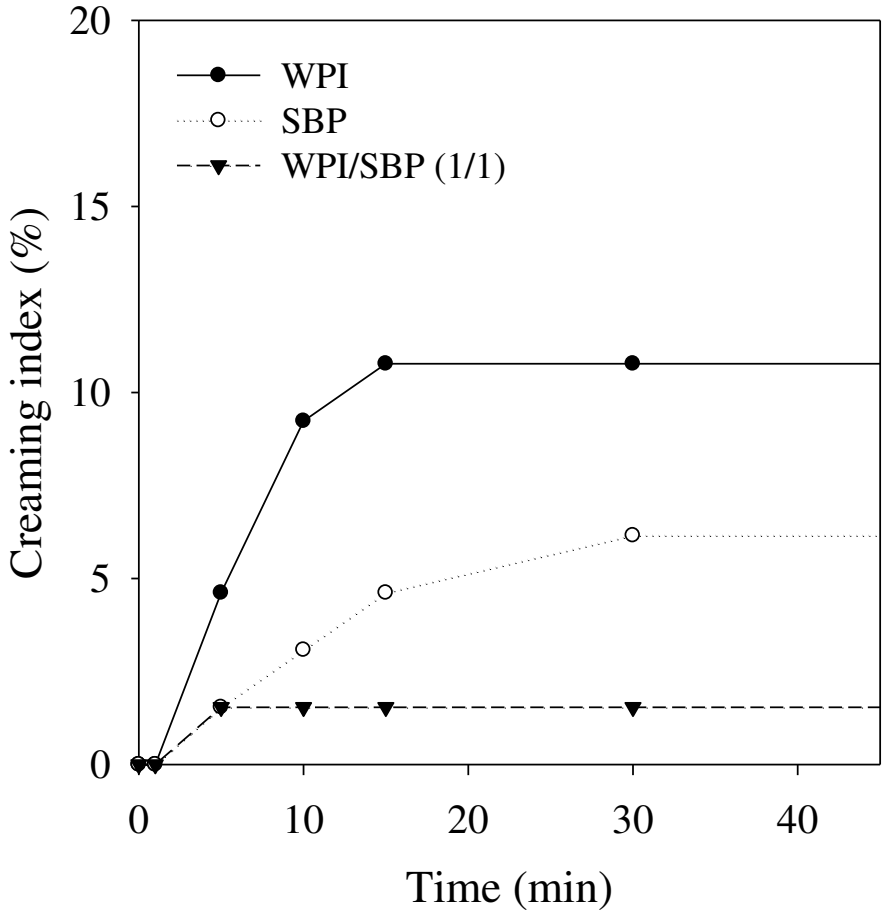

Fig 5 Accelerated creaming test of decane-in water emulsions containing whey protein isolate (WPI), sugar beet pectin (SBP) or their complex (WPI/SBP) in a ratio 1/1, was performed by centrifugation at 2,500 rpm during 0, 5, 15, 20, 30 and 45 min. Samples were diluted till reach an 1% *w/w* of decane.

a

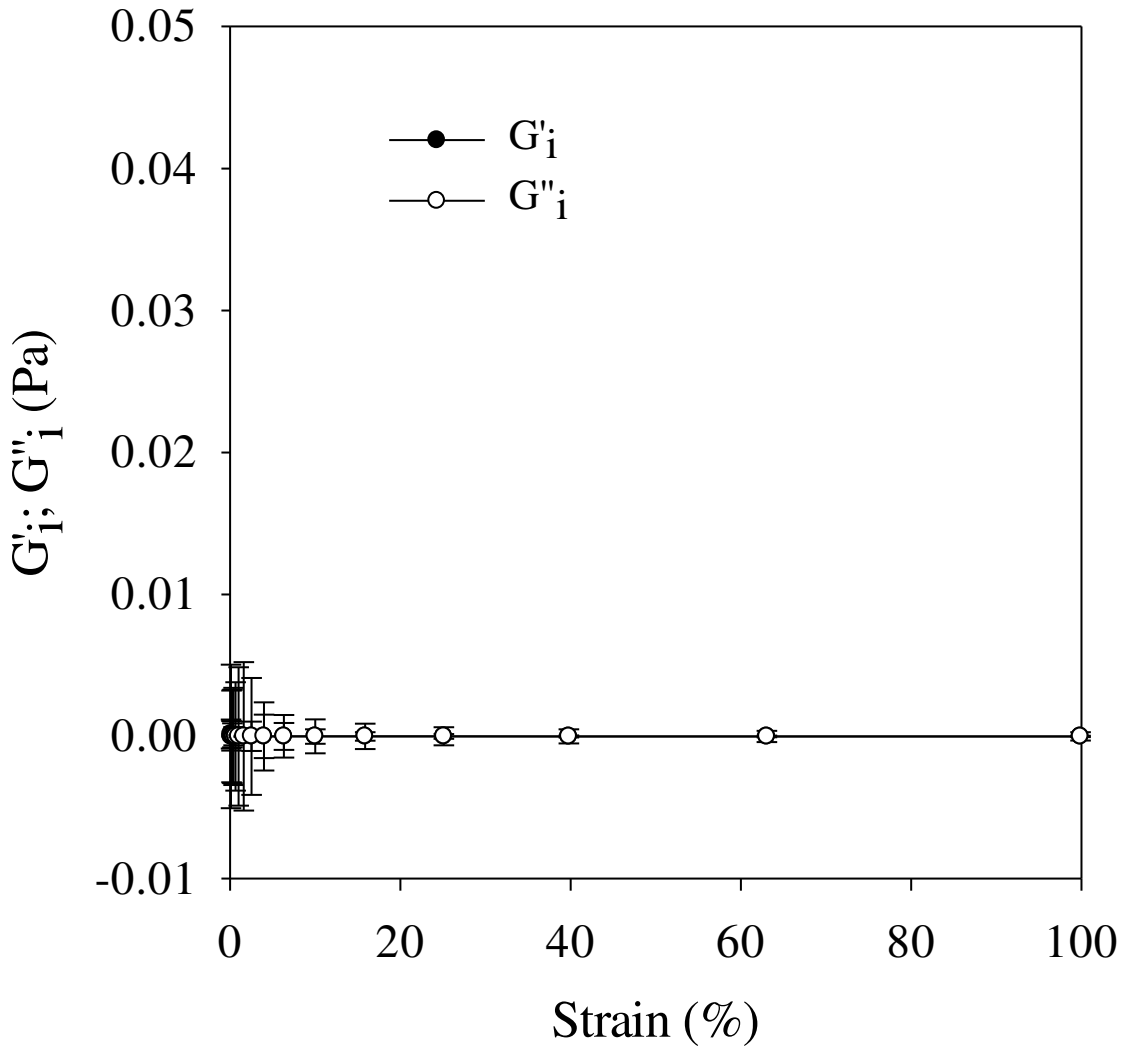

b

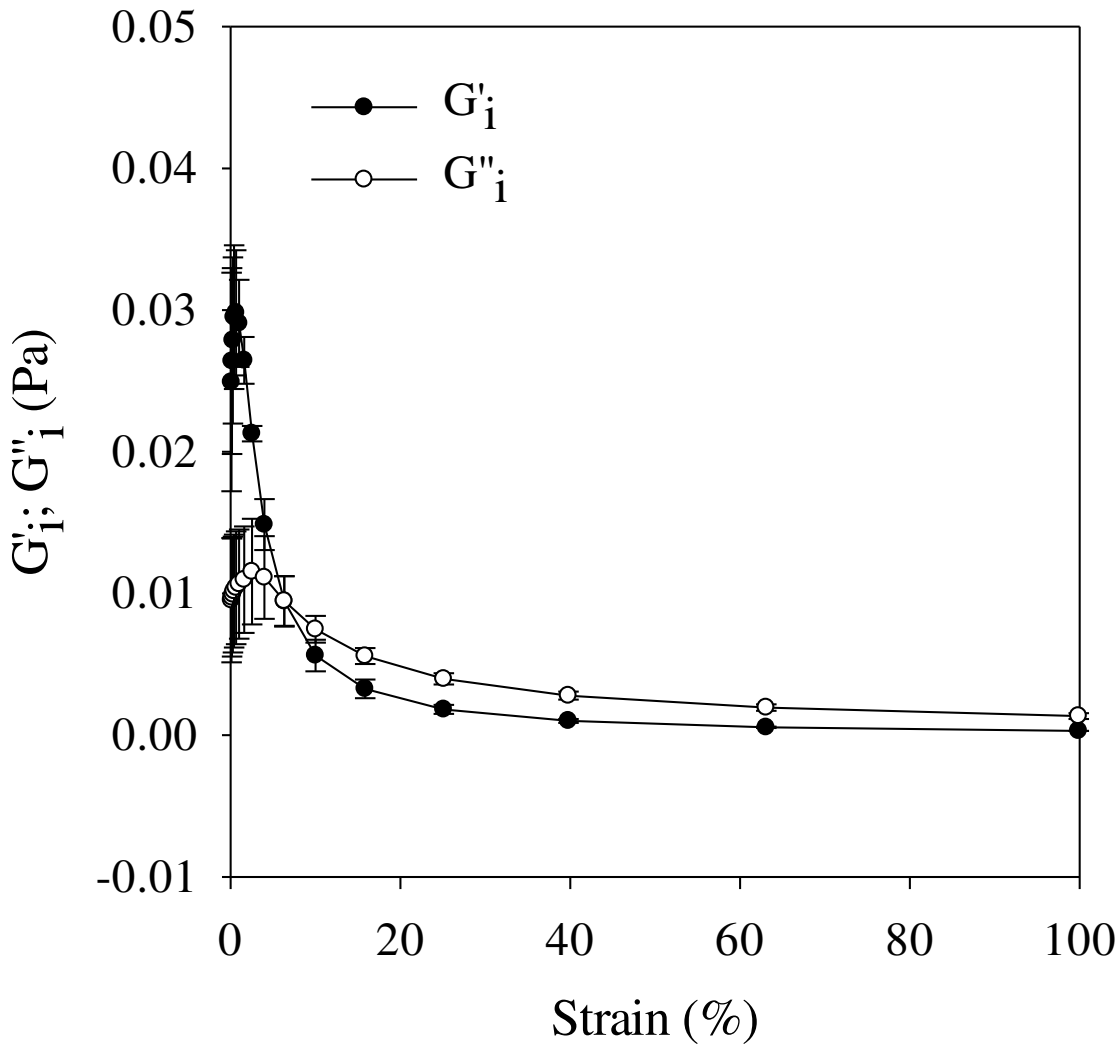

c

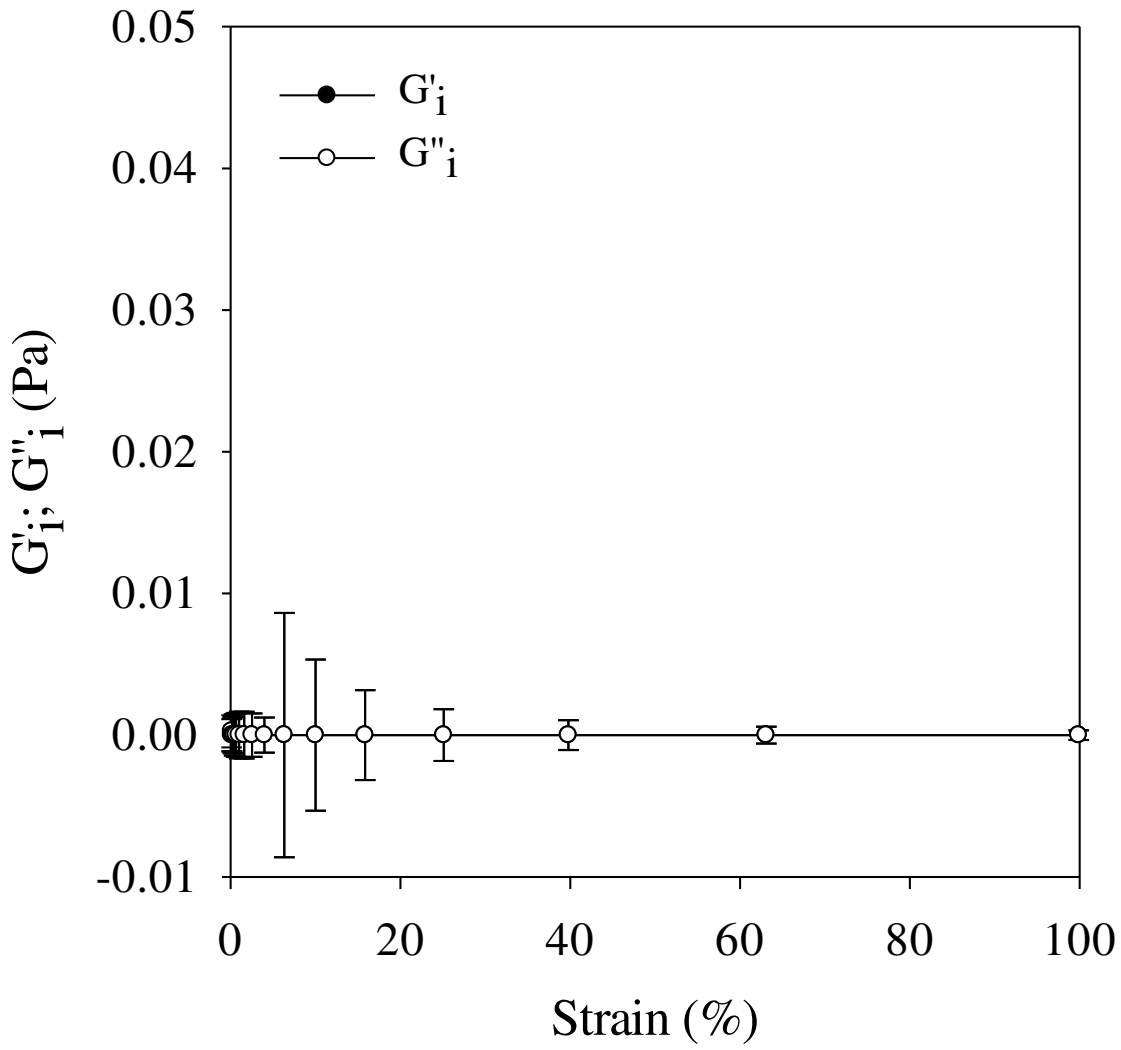

Fig 6 Interfacial rheology of (**a**) whey protein isolate (WPI), (**b**) sugar beet pectin (SBP) or (**c**) their complex (WPI/SBP) in a ratio of 1/1 solutions at the water-decane interface.

Table 1. Decane-in water nanoemulsions physicochemical properties in terms of the mean droplet diameter over volume ($d_{4;3}$ in μm and ζ-potential (mV).

	$d_{4;3}$ (μm)	d_{10} (μm)	ζ-potential (mV)
2% *w/w* WPI; 20% *w/w* decane	0.31 ± 0.03^{AB}	0.129 ± 0.003^{A}	37.5 ± 0.3^{A}
2% *w/w* SBP; 20% *w/w* decane	0.37 ± 0.09^{A}	0.15 ± 0.09^{B}	-22.1 ± 0.5^{B}
2% *w/w* WPI/SBP (1/1) complex; 20% *w/w* decane	0.26 ± 0.07^{B}	0.11 ± 0.01^{AB}	-20.4 ± 0.5^{C}

^{A,B,C} Means in the same column with different letters are significantly different ar $p < 0.05$ in terms of comparing different biopolymers as emulsifiers.

Table 2. Radius (μm) and density (g/cm^3) of decane-in water nanoemulsions as well as the number and volume (cm^3) of oil droplets necessary to calculate the mass (m_{shell}) in grams, volume (V_{shell}) in cm^3 and densities of the shell (g/cm^3) through equations 1-6; for 100 g of nanoemulsion, 2 g of biopolymer solution and 20 g of decane, whose density is 0.734 g/cm^3 and hence, the oil volume ($V_{total\ oil}$) equals $27.3 \pm 1.8 \cdot 10^{-3}$ cm^3.

	$r_{4;3}$ (μm)	$\rho_{emulsion}$ (g/cm^3)	Number of doplets	$V_{oil\ droplet}$ (cm^3)	m_{shell} (g)	V_{shell} (cm^3)	ρ_{shell} (g/cm^3)
WPI	0.16 ± 0.03	$0.950 \pm 5 \cdot 10^{-5}$	$1.7 \cdot 10^{15}$	$1.6 \cdot 10^{-14} \pm 1 \cdot 10^{-16}$	$1.2 \cdot 10^{-15} \pm 2.6 \cdot 10^{-17}$	$4.6 \cdot 10^{-14} \pm 1.2 \cdot 10^{-16}$	$0.026 \pm 2 \cdot 10^{-4}$
SBP	0.19 ± 0.09	$0.967 \pm 2 \cdot 10^{-4}$	$9.4 \cdot 10^{14}$	$2.9 \cdot 10^{-14} \pm 9.6 \cdot 10^{-16}$	$2.1 \cdot 10^{-15} \pm 1.5 \cdot 10^{-18}$	$8.1 \cdot 10^{-14} \pm 9.6 \cdot 10^{-16}$	$0.026 \pm 8 \cdot 10^{-4}$
WPI/SBP (1/1) complex	0.11 ± 0.07	$0.943 \pm 1 \cdot 10^{-4}$	$5.3 \cdot 10^{15}$	$5.1 \cdot 10^{-15} \pm 1.3 \cdot 10^{-15}$	$3.8 \cdot 10^{-16} \pm 10 \cdot 10^{-21}$	$1.5 \cdot 10^{-14} \pm 1.3 \cdot 10^{-15}$	$0.025 \pm 4 \cdot 10^{-3}$

Universitat de Lleida
Departament de Tecnologia d'Aliments

Av. Alcalde Rovira Roure, 191
E 25198 LLEIDA (Catalunya)
Tel. +34 973 70 25 21
tecal.secretaria@udl.cat
www.tecal.udl.cat

Lleida, 16-10-2019

Subject: Submission of original manuscript

Dear Editor,

Please find attached the original research paper entitled *Protein: polysaccharide complexes to stabilize decane-in-water nanoemulsions* by María Artiga-Artigas, Corina Reichert, Laura Salvia-Trujillo, Benjamin Zeeb, Olga Martín-Belloso and Jochen Weiss.

Ostwald ripening is one of the most common destabilization phenomena in nanoemulsions, especially those containing short-chain oils such as alkanes. Proteins and polysaccharides have been commonly used as emulsifier of short-chain oils-loaded nanoemulsions as an alternative of using synthetic surfactants. However, in several cases, the emulsifying capacity of these biopolymers is not sufficient to prevent Ostwald ripening. Therefore, we hypothesize that the preparation of stronger interfaces may enhance nanoemulsions stability by preventing or avoiding Ostwald ripening. In this regard, whey protein isolate (WPI) and sugar beet pectin (SBP) complexes formed by electrostatic interactions, as well as both biopolymers alone were used to form and stabilize interfacially structured nanoemulsions containing decane. Moreover, interfacial rheology measurements were conducted to study the adsorption of the biopolymers alone and the complexes. Nanoemulsions were stored for 21 days at room temperature to assess their stability against Ostwald ripening over time. Complexes showed higher emulsifying capacity than biopolymers alone since particle size of complex-stabilized nanoemulsions remained stable for at least 48 h after preparation, whereas WPI- or SBP-stabilized nanoemulsions were prone to destabilization during the first 24 h. This work provides new information about the behavior of WPI: SBP complexes as emulsifiers for short-chain oils-loaded nanoemulsions. Results evidenced that the protein fraction may be adsorbed at the oil interface thus dominating the interface rheology, whereas pectin chains located on the periphery of the complex and oriented towards the water phase. The resultant WPI: SBP complex-stabilized nanoemulsions can effectively be used as carriers of short-chain oils including essential oils.

The authors believe that this manuscript provides relevant insight into the formation of complex-stabilized nanoemulsions more resistant to Ostwald ripening than those single-stabilized. We hope that this article satisfies the requirements of *Food Biophysics* and that you might consider it for publication in this Journal. Please do not hesitate to contact us for any further eventuality.

We looking forward to hearing from your earliest news.

Yours sincerely,

María Artiga-Artigas

maria.artiga@udl.cat